Original Research

Tantalum coating of porous carbon scaffold supplemented with autologous bone marrow stromal stem cells for bone regeneration *in vitro* and *in vivo*

Xiaowei Wei[1], Dewei Zhao[1], Benjie Wang[1], Wei Wang[1], Kai Kang[1], Hui Xie[1], Baoyi Liu[1], Xiuzhi Zhang[1], Jinsong Zhang[2] and Zhenming Yang[2]

[1]Department of Orthopaedic Laboratory, Zhongshan Hospital of Dalian University, Dalian 116001, China; [2]Institute of Metal Research, Chinese Academy of Sciences, Shenyang 110016, China
Corresponding author: Dewei Zhao. Email: zhaodewei2000@163.com

Abstract

Porous tantalum metal with low elastic modulus is similar to cancellous bone. Reticulated vitreous carbon (RVC) can provide three-dimensional pore structure and serves as the ideal scaffold of tantalum coating. In this study, the biocompatibility of domestic porous tantalum was first successfully tested with bone marrow stromal stem cells (BMSCs) *in vitro* and for bone tissue repair *in vivo*. We evaluated cytotoxicity of RVC scaffold and tantalum coating using BMSCs. The morphology, adhesion, and proliferation of BMSCs were observed via laser scanning confocal microscope and scanning electron microscopy. In addition, porous tantalum rods with or without autologous BMSCs were implanted on hind legs in dogs, respectively. The osteogenic potential was observed by hard tissue slice examination. At three weeks and six weeks following implantation, new osteoblasts and new bone were observed at the tantalum–host bone interface and pores. At 12 weeks postporous tantalum with autologous BMSCs implantation, regenerated trabecular equivalent to mature bone was found in the pore of tantalum rods. Our results suggested that domestic porous tantalum had excellent biocompatibility and could promote new bone formation *in vivo*. Meanwhile, the osteogenesis of porous tantalum associated with autologous BMSCs was more excellent than only tantalum implantation. Future clinical studies are warranted to verify the clinical efficacy of combined implantation of this domestic porous tantalum associated with autologous BMSCs implantation and compare their efficacy with conventional autologous bone grafting carrying blood vessel in patients needing bone repairing.

Keywords: Bone marrow stromal stem cells, porous tantalum, biocompatibility, osteogenesis, bone tissue engineering

Experimental Biology and Medicine **2016; 241: 592–602. DOI: 10.1177/1535370216629578**

Introduction

Bone defect is a kind of bone loss caused by bone trauma, infection, tumor resection, and other systemic diseases.[1,2] The body can regenerate and repair small-area bone defect but is unable to repair large-area bone defect.[3,4] Allogeneic bone grafting is related to immune rejection and cannot construct effective blood supply.[5] Autologous bone grafting is one of the common methods of bone defect reconstruction.[6] But this strategy may sometimes result in complications and deformities in the donor area where bone mass is limited.[7] However, the most important disadvantage of autologous bone grafting is that the permanent blood supply cannot be steadily constructed. So the bone graft might undergo fibrosis in the process of ''creeping substitution'' and might be absorbed at the end. At present, the most effective method for treating bone defect is autologous bone grafting carrying blood vessel.[8,9] This method can prevent bone graft to be absorbed and could reconstruct blood supply permanently, but there are also some disadvantages related to this strategy including inadequate bone resource, limited bone shape, inducing some damage in the donor area, etc. It is to note that autologous bone grafting carrying blood vessel cannot repair the large bone defect.

Cancellous bone has porous network structure consisted by a large number of interconnected trabecular. Trabecular connecting with cortical bone owns irregular three-dimensional network structure in the bone marrow cavity, forming a sponge-like structure to support the hematopoietic tissue in cancellous bone. In the past two decades, there were numerous reports and researches on artificial porous materials for bone defect, highlighting the clinical importance of research in this field. Ideal scaffold for bone defect should

have not only good biocompatibility, but also a porous framework within which revascularization occurs and against which new bone is layered and can be developed as substitutes of trabecular.[10] The most commonly used substance of porous biomaterials is calcium hydroxyapatite (HA) which is the main chemical constituent of bone.[11] However, HA implants might undergo some degree of chemical dissolution, thus limiting their clinical use. Other commonly used porous materials are ceramic, polymers, metals, and so on. Ceramics is strong but very brittle. Polymers have good ductility but are very weak. Metals with high strength and good ductility become attractive candidate for implants. But most metals and alloys currently available are subject to corrosion in the biological environment.[12]

Tantalum metal has good ductility, tenacity and biocompatibility, and is highly resistant to corrosion but does not result in body tissues stimulation. Solid tantalum has been considered as a good substrate for the attachment, growth, and differentiated function of human osteoblasts.[13] Sagomonyants KB and Welldon KJ, respectively, reported that porous tantalum stimulated the proliferation and osteogenesis of osteoblasts from elderly women patients and from patients with total joint replacement surgery.[14,15] Porous tantalum medical product made by Zimmer corporation in the USA has been successfully applied to the hip, knee, shoulder, ankle joint, and the spinal surgery.[16–21] Nevertheless, melting point of tantalum is about 3000°C, so porous tantalum with highly interconnected pores and uniform honeycomb structure is very difficult to obtain through the traditional technology. Until now, Zimmer is the only medical device company with porous tantalum in the world.

The preparation of porous tantalum was always a problem in the past decades. Because the density of tantalum is too high, a kind of low density and non-toxic porous scaffold need to be sprayed on tantalum in order to reduce the density of porous tantalum. Carbon is a non-toxic material with excellent biocompatibility.[22] Qiu *et al.* used carbon fiber to repair osteochondral defects in the rabbit knee, and better subsurface support was noticed by carbon fiber than in the case of natural healing.[23] Reticulated vitreous carbon (RVC) containing more than 99% carbon element owns highly interconnected pores and honeycomb structure.[24] The microstructure and pore size of RVC is very similar to natural cancellous bone. In 2009, Aoki *et al.* found that thin carbon fiber web as bone substitute materials with human bone morphogenetic protein-2 promoted the formation of new heterotopic bone in mice back muscles.[25] However, RVC is brittle and easy to crack because of its low mechanical strength, a metal coating is essential in order to gain sufficient mechanical strength and suitable elastic modulus. The combination of RVC and tantalum coating might thus provide a scaffold for reconstruction of blood supply, growth of new bone, and become a kind of artificial porous medical material.

Autologous bone marrow stromal stem cells (BMSCs) are considered as the ''best seed cells'' due to their wide sources, easy extraction, and fast proliferation characteristics. BMSCs can transform into osteoblasts and promote bone repair.[26] Our previous study demonstrated the efficacy and safety of autologous implantation of *ex vivo* expanded BMSCs into the femoral head for the treatment of early stage osteonecrosis of the femoral head.[27] Stiehler *et al.* reported that human mesenchymal stem cells cultured on solid tantalum plate had nice osteogenic differentiation.[28] In recent years, studies on porous material co-cultured with ''seed cells'' become a hot spot in the field of bone tissue engineering.[29] It was shown that biological materials combined with BMSCs *in vivo* can improve osteogenesis and accelerate bone formation and bone integration with the material.[30] Meanwhile, many researchers have reported the biocompatibility of various porous materials with primary culture BMSCs isolated from small animals such as mice, rats, or rabbits.[31,32] But there is scarcely study on the biocompatibility and osteogenic potential of porous tantalum with primary culture BMSCs isolated from large animals.

In this study, we tested the biocompatibility of tantalum coating and RVC scaffold with canine BMSCs adhesion and proliferation *in vitro* and osteogenic potential of porous tantalum associated with autologous on bone defect repair *in vivo*. The aim of this work was to assess the possibility of application of tantalum coating of RVC scaffold supplemented with autologous BMSCs for bone regeneration.

Materials and methods

Preparation of RVC and porous tantalum

RVC and porous tantalum were produced by Institute of Metal Research, Chinese Academy of Sciences and Zhongshan Hospital of Dalian University, respectively. The preparation method of porous tantalum has been approved as an invention patent in China (No. ZL 2013 1 0447227.6; http://www.sipo.gov.cn/). Briefly, RVC scaffold was etched in 10% hydrochloric acid for 10 min and then cleaned in ddH_2O and ethanol, respectively. The scaffold then was put into the reaction chamber after drying with nitrogen. Next, $TaCl_5$ powder which was heated to 150°C was sucked into the reaction chamber with high temperature argon gas (300°C) as the carrier gas. The carrier gas flow rate was 100 mL/min; the temperature in reaction chamber was 1050°C; the pressure in reaction chamber was 10 Pa. At the same time, reduction reaction in reaction chamber lasted for 4 h with 120 mL/min hydrogen flow rate. The physical and mechanical properties of domestic porous tantalum were shown in Table 1.

Isolation and culture of BMSCs

All procedures on animals were approved by the Animal Ethics Committee of Dalian University. Use of animals was approved by the Institution's Animal Care and Use Committee. BMSCs were obtained from eight-week-old male Beagle dogs by centrifugal isolation. Whole bone marrow was pooled and resuspended in DMEM/F12 (Hyclone, Thermo Fisher Scientific, Waltham, MA, USA), supplemented with 10% FBS (Hyclone, Thermo Fisher Scientific, Waltham, MA, USA), 100 UI/mL penicillin (Invitrogen, Life Technologies, Carlsbad, CA, USA),

Table 1 Pore size, porosity, and mechanical properties of porous tantalum

Sample	All pore mean size (μm)	Open porosity (%)	Tantalum coating thickness (μm)	Compressive strength (MPa)	Young's modulus (GPa)
Porous tantalum	150–400	70–85	40–60	35–100	10–30

100 μg/mL streptomycin (Invitrogen, Life Technologies, Carlsbad, CA, USA), and seeded on cell culture plastic. Cells were maintained at 37°C under 5% CO_2 in humidified air. After two days, cultures were rinsed carefully with phosphate buffer saline (PBS) to remove non-adhered cells and cultured in fresh culture medium. After 10–12 days, the cells reached about 90% confluence for subsequent experimental studies.

Flow cytometry

Cells were washed with PBS and then harvested and counted. 5×10^5 cells in 100 μL PBS were incubated with 5 μL FITC-conjugated rat anti-dog CD44 (0.2 mg/mL), 5 μL PE-conjugated mouse anti-dog CD34 (0.2 mg/mL), or 5 μL PE-conjugated mouse anti-dog CD45 for 15 min, respectively. The negative control was generated by replacing the antibody with isotype IgG. After washing with PBS containing 1% BSA (Sigma-Aldrich, St. Louis, MO, USA), fluorescence of cells was analyzed using a Coulter EPICS XL flow cytometer (Beckman Coulter, Fullerton, CA).

Direct immunofluorescence staining

After washing with PBS, cells grown on coverslips were fixed in 4% paraformaldehyde (Sigma-Aldrich, St. Louis, MO, USA) for 20 min. After blocked with 3% complete serum for 2 h at 37°C, cells were incubated with FITC-conjugated CD44 (1:200 dilution), PE-conjugated CD34 (1:200 dilution), or PE-conjugated CD45 (1:200 dilution) for 30 min. The negative control was generated by replacing the antibody with isotype IgG. After several rinses with PBS, cells were incubated with 4′,6-diamidino-2-phenylindole (DAPI) (Sigma-Aldrich, St. Louis, MO, USA) for 30 min. Images were captured with the Olympus BX51 fluorescence microscope.

Proliferation assay by MTT chromatometry

1.0×10^7/L, 3.0×10^7/L, 9.0×10^7/L BMSCs were seeded in wells of a 96-well plate with DMEM/F12, respectively. Cells were allowed to precipitate at 37°C for 1 h and then an autoclaved RVC or porous tantalum was added with sterile forceps to each well. After one, three, five, and seven days of co-culture, porous tantalum or its scaffold (RVC) was removed and relative cell numbers were detected by MTT chromatometry (Sigma-Aldrich, St. Louis, MO, USA), respectively. Briefly, 20 μL tetrazolium (5 mg/mL, Sigma-Aldrich, St. Louis, MO, USA) was added after incubation. Four hours later, the MTT solution was removed, the formed formazan crystals were dissolved in 200 μL DMSO (Sigma-Aldrich, St. Louis, MO, USA) for 10 min and absorbance was measured at 490 nm.[24]

Scaffold cell loading and fluorescence labeling

The autoclaved RVC scaffolds were submerged in PBS to reduce liquid rejection by electrostatic loading. The excess fluid around the scaffold was aspirated. Then 50 μL of BMSC suspension culture medium (1×10^6 cells/mL) were loaded onto each RVC scaffold. The constructs were then incubated for 2 h in the CO_2 incubator at 37°C. Medium was changed every 3–4 days. After 28 days of co-culture, scaffolds were rinsed with PBS, fixed with 4% paraformaldehyde overnight at 4°C, rinsed with PBS, and permeabilized with 0.2% Triton X-100 in PBS for 30 min at room temperature, followed by another rinse with PBS. Then cells were labeled at room temperature under light protection for 15 min with a PI (Sigma-Aldrich, St. Louis, MO, USA) in PBS at a concentration of 5 μg/mL and again rinsed with PBS. Images were captured with the Nikon confocal microscope.

Adhesion and growth of BMSCs on RVC scaffold or porous tantalum by scanning electron microscopy (SEM)

The autoclaved RVC or porous tantalum was submerged in PBS to reduce liquid rejection by electrostatic loading. The excess fluid around the scaffold was aspirated. Then 200 μL of BMSC suspension culture medium (4×10^6 cells/mL) were loaded onto RVC or porous tantalum. The constructs were incubated in the 5% CO_2 incubator at 37°C. Medium was changed every 2–3 days. After seven, 14, 21, and 28 days of co-culture, materials were rinsed with PBS, fixed with 2% glutaraldehyde for 2 h, rinsed with PBS. Then the two materials were infiltrated, respectively, in 50, 70, 80, 90, 100% dehydrated alcohol at all levels to make BMSCs dehydration. Then samples were dried at critical point and one surface of each sample was sprayed with gold *in vacuo* and examined by SEM in a JEOL (Tokyo, Japan) JSM-6360LV instrument.

Animals and implantation

This experimental protocol was performed in accordance with the China Animal Research Guidelines, and all procedures on animals were approved by the Animal Ethics Committee of Dalian University. All surgery was performed under sodium pentobarbital anesthesia, and all efforts were made to minimize suffering. After male Beagle dogs (male, 12 weeks old, 8.5–10 kg) were anesthetized, 1.0 cm × 0.7 cm bone defect cylinder was made in bilateral hind legs' greater trochanter along the direction of femur. Then, 0.9 cm × 0.6 cm porous tantalum rods with or without BMSCs were implanted in defect sites, respectively. In porous tantalum rods with BMSCs group, 200 μL

of BMSC suspension culture medium at a concentration of 5×10^7 cells/mL were loaded onto porous tantalum for one week *in vitro* before implantation. X-ray was used in order to show the position of tantalum at three, six, and 12 weeks postimplantation (three specimens per sampling time point). In defect with BMSCs group, 200 μL of BMSC suspension culture medium at a concentration of 5×10^7 cells/mL were injected into the defect site. The defect group without BMSCs served as untreated control group. Sampling time point for the untreated control group, defect with BMSCs group, and normal control group was at 12 weeks post various treatments. At the study end, dogs were anesthetized and sacrificed in order to gain the bilateral greater trochanter samples. For the subcutaneous pocket site, porous tantalum with the connective tissue was obtained at 12 weeks postimplantation.

Histomorphology

Defect bearing including greater trochanter and subcutaneous pocket was prepared for histological evaluation. Samples were fixed in 10% formaldehyde in phosphate buffer (pH 7.4). Bones were dehydrated in a graded series of ethanol and embedded in plastic for hard tissue slicing. Sections of 10 μm thickness were prepared throughout the defect/tantalum sites for Van Gieson's stain. Briefly, the sections were put into methanoic acid for 3 min and then in methanol for 2 h. After washing in $dddH_2O$, sections were incubated with methylene blue (Sigma-Aldrich, St. Louis, MO, USA) for 5 min at 60°C. After several rinses with $dddH_2O$, sections were stained by fuchsin-picric acid (Sigma-Aldrich, St. Louis, MO, USA) for 15 min. Slides were washed by dehydrated alcohol and then visualized at 40× and 100× magnification on an inverted microscope (Olympus, Tokyo, Japan). Five visual fields on each slice were selected randomly and taken pictures under 100 × magnification optical microscope. New bone formation area in the pores of porous tantalum was measured by Image J software.

Statistical analysis

Each experiment was repeated for three times, results presented as the mean ± SEM. Statistical differences between test groups were analyzed by one-way ANOVA and LSD *post hoc* test. A p *value* <0.05 was considered statistically significant.

Results

Identification of BMSCs

The isolated cells expressed the MSC marker CD44 (Figure 1(a)) but scarcely expressed the hematopoietic stem cells marker CD34 (Figure 1(b)) and leukocyte marker CD45 (Figure 1(c)). The isolated cells expressed CD44 protein with green fluorescence in cell membrane and cytoplasm (Figure 1(d)), while the cells were negative for CD34 and CD45 so just nuclei was stained with blue fluorescence of DAPI (Figure 1(e) and (f)). These expression patterns in dog are similar to BMSCs in human.[33]

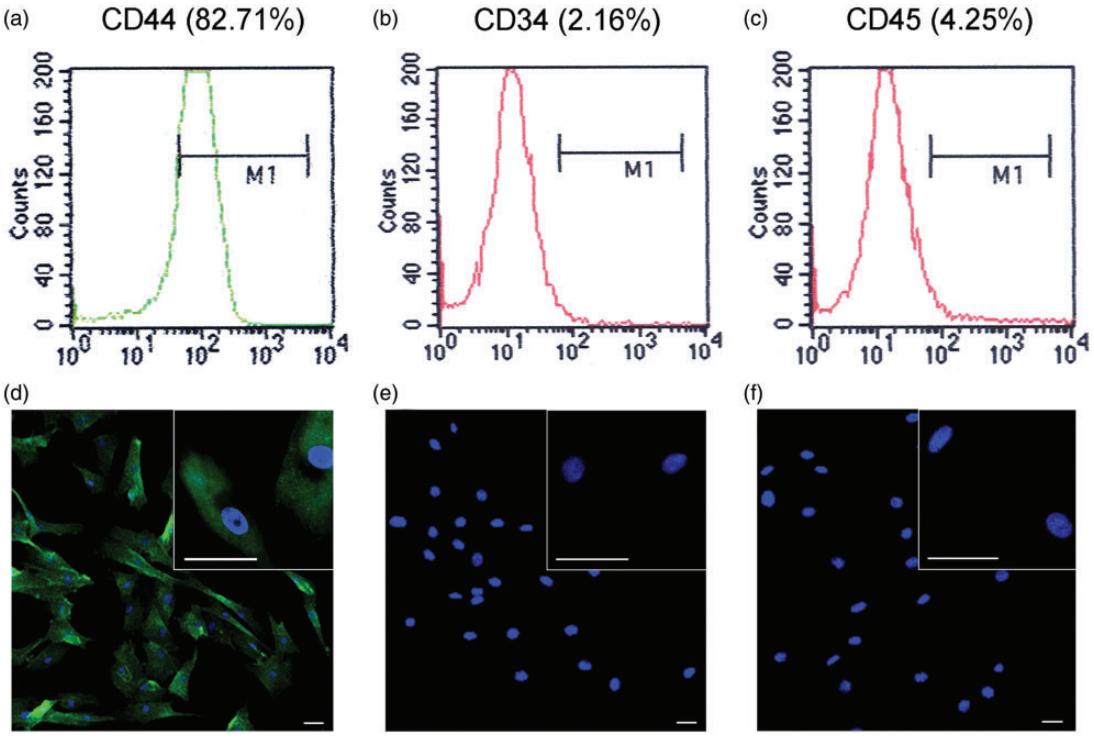

Figure 1 Identification of BMSCs in the third subculture passage by flow cytometry and immunofluorescence. BMSCs were identified with the surface markers (a) $CD44^+$ (82.71%), (b) $CD34^-$ (2.16%), and $CD45^-$ (4.25%). The isolated cells expressed CD44 protein with green fluorescence in cell membrane and cytoplasm (d), while the cells were negative for CD34 (e) and CD45 (f). Bar=50 μm

Proliferation of BMSCs on porous tantalum or RVC scaffold

The statistical results showed that the proliferation of BMSCs co-cultured with porous tantalum or RVC for one, three, five, and seven days, respectively, was not inhibited compared to the control group ($P > 0.05$) (Figure 2). So we considered that BMSCs didn't suffered cytotoxicity in the presence of domestic porous tantalum or RVC.

Adhesion and growth of BMSCs on porous tantalum or RVC scaffold

After 48 h, adherent cells from primary culture system presented with round, oval, or polygonal shapes, some of them started to stretch. After 10 days, BMSCs reached about 90% confluence (Figure 3(a)). After 28 days of co-culture, dense populations of BMSCs with red fluorescence were visualized to adhere on the RVC material under confocal microscopy. Round, partially spread, and also fully spread BMSCs were also observed (Figure 3(b)). Energy spectrum showed that the component of RVC was carbon element (Figure 3(c)).

SEM results were as follows. BMSCs cultured on RVC for seven days; there were few BMSCs on RVC surface and the morphology of BMSCs presented as long spindle shape (Figure 3(d)). After 14 days, BMSCs presented with diverse shapes and dispersed on the surface of RVC scaffolds and there was no connection among cells (Figure 3(e)). After 21 days, polygonal BMSCs were seen and connected with each other and exhibited a fully spread phenotype (Figure 3(f)). After 28 days, there were more adherent and spread BMSCs compared to that after 21 days co-culture (Figure 3(g)).

Energy spectrum showed that the component of porous tantalum was tantalum element and carbon element (Figure 4(a)). Several BMSCs on porous tantalum surface could be visualized after seven days BMSCs culture on porous tantalum (Figure 4(b)). After 14 days, BMSCs began to connect with each other and exhibited a fully spread phenotype (Figure 4(c)). After 28 days, the number of adherent BMSCs was significantly higher than that post 21 days co-culture (Figure 4(d) and (e)). Overall, adhesion and spread of BMSCs on porous tantalum were better than on RVC scaffold at comparable culture time point.

Imageology and histological evaluation of porous tantalum

Biocompatibility of porous tantalum in subcutaneous pocket. As we know, massive fibrillar connective tissue will be generated around the defect sites for large-area bone defect. The connective tissue is the main component of subcutaneous pocket under the canine groin. To observe the biocompatibility of porous tantalum with loose connective tissue and dense connective tissue, porous tantalum was implanted into subcutaneous pocket under the canine groin (Figure 5(a)). After 12 weeks, porous tantalum was surrounded by the connective tissue without local tumor formation and inflammatory reaction (Figure 5(b)). Van Gieson's stain results showed that subcutaneously implanted porous tantalum was completely integrated into the connective tissue without immunologic rejection (Figure 5(c)).

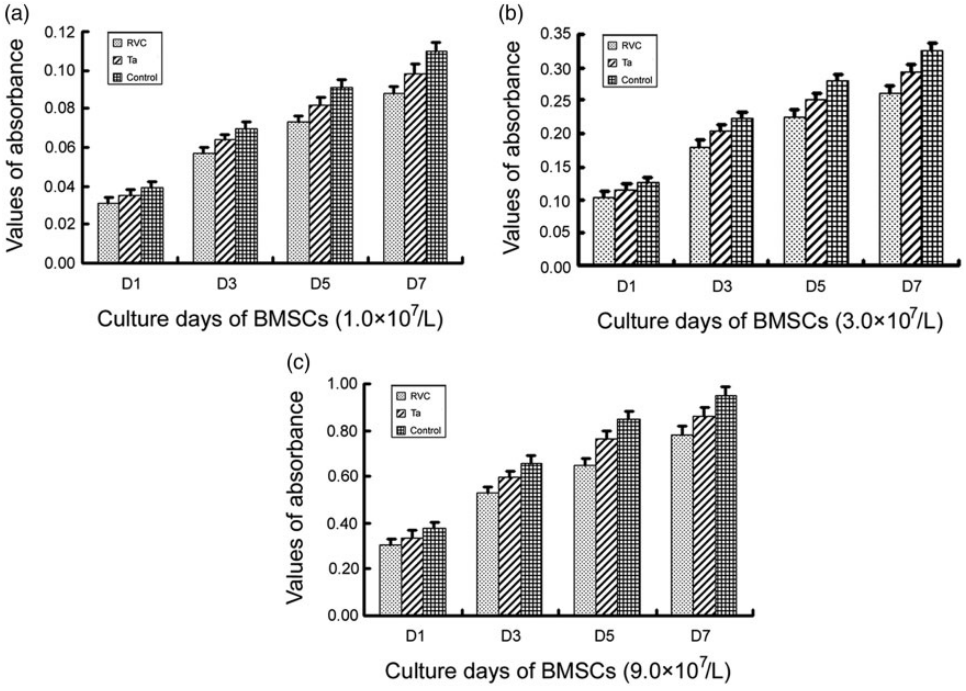

Figure 2 BMSCs proliferation on the surface of porous tantalum or RVC scaffold. 1.0×10^7/L, 3.0×10^7/L, 9.0×10^7/L bone marrow stromal stem cells were seeded in wells of a 96-well plate with DMEM/F12 medium, respectively. The proliferation of BMSCs was assessed by MTT assay (measures of optical density at 490 nm). BMSCs were co-cultured with the RVC material for one, three, five, and seven days. Then MTT assays were done with tetrazolium and DMSO. Data were presented as the mean ± SEM. This experiment was repeated for three times

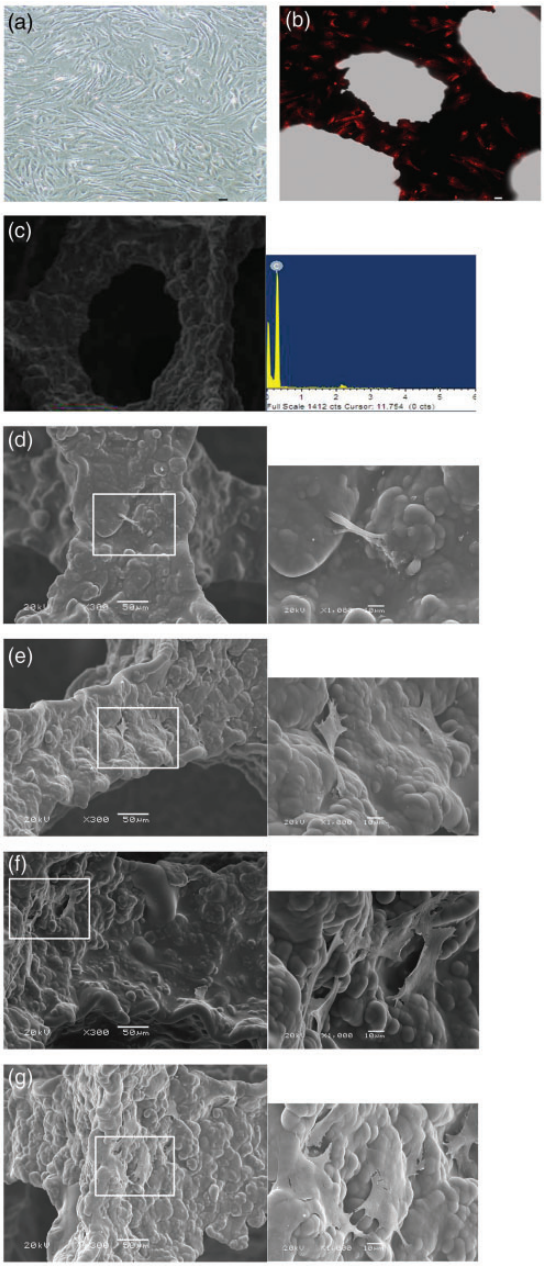

Figure 3 Morphology of BMSCs cultured on RVC scaffold observed by confocal microscopy and SEM. Light microscopy image of BMSCs in the third passage (a). Confocal microscopy image of propidium iodide-stained BMSCs co-cultured with the RVC material for 28 days (b). Bar = 30 μm. The component of RVC analyzed by energy spectrum (c). Canine bone marrow stromal stem cell and RVC scaffold were co-cultured for seven days (d), 14 days (e), 21 days (f), and 28 days (g). Big image was magnified 300 ×, bar = 50 μm; small image was magnified 1000 ×, bar = 10 μm. (A color version of this figure is available in the online journal.)

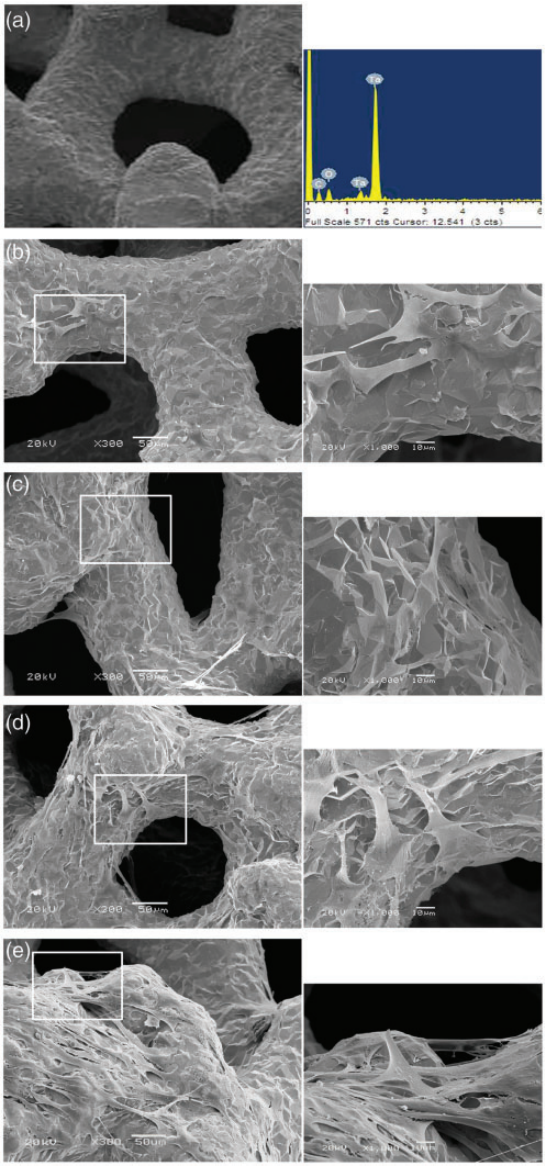

Figure 4 Morphology of BMSCs cultured on porous tantalum observed by SEM. The component of porous tantalum analyzed by energy spectrum (a).Canine BMSCs and porous tantalum were co-cultured for seven days (b), 14 days (c), 21 days (d), and 28 days (e). Big image was magnified 300 ×, bar = 50 μm; small image was magnified 1000 ×, bar = 10 μm. (A color version of this figure is available in the online journal.)

Osteogenesis of porous tantalum associated with autologous BMSCs. Three weeks postimplantation of porous tantalum rods without BMSCs, massive fibrillar connective tissue formation was observed in the pore of tantalum rods (Figure 6(a)). Three weeks postimplantation of porous tantalum rods associated with autologous BMSCs, horizontal section imaging showed that new bone tissue grew at the interface of the porous tantalum and the host bone. Meanwhile, new bone tissue and fibrillar connective tissue were observed on the surface of the tantalum rods and in the pores (Figure 6(b)). By six weeks, the number of new bone cells was seen at the interface and connected with the host bone with porous tantalum implantation alone. In addition, the tantalum surface and pores were covered with new bone tissue (Figure 6(c)). While defect area was filled with much more new bone tissue in the pore of scaffold postimplantation of porous tantalum rods associated with autologous BMSCs (Figure 6(d)). At 12 weeks postporous tantalum implantation alone, porous tantalum was completely filled with calcification bone tissue (Figure 6(e)). Interestingly, at 12 weeks postporous tantalum implantation plus autologous BMSCs, regenerated trabecular

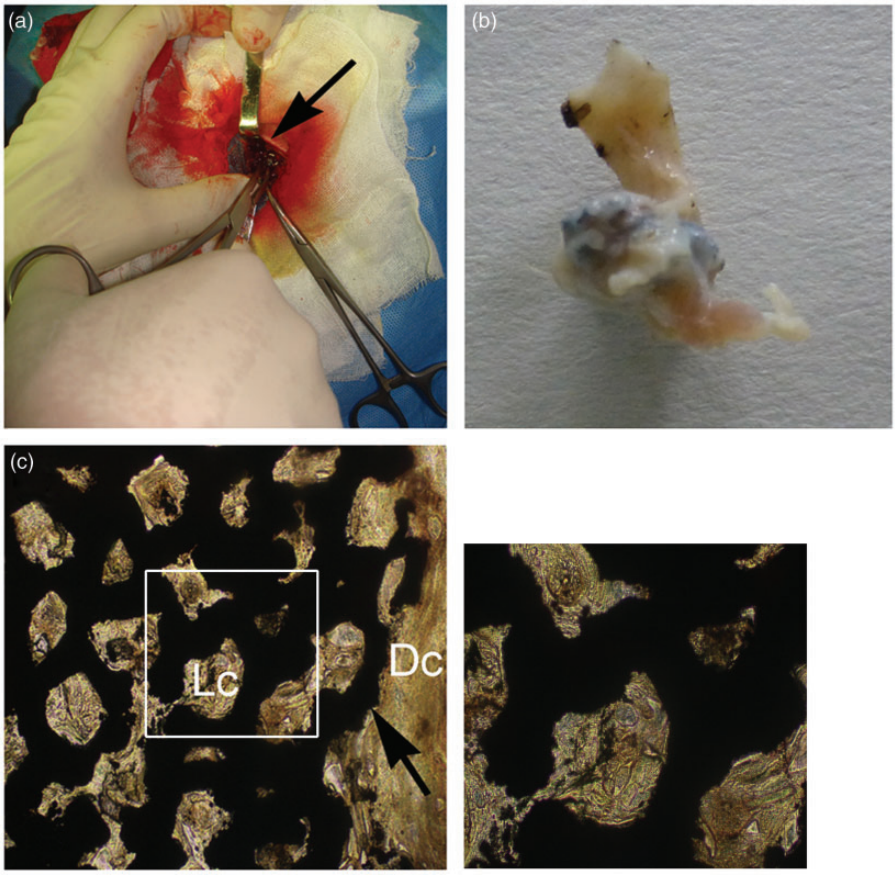

Figure 5 Tissue compatibility of porous tantalum in canine subcutaneous pocket. Porous tantalums (black arrows) are associated with the voids left from the implant. Porous tantalum was implanted at subcutaneous pocket (a) and taken out after 12 weeks (b). (c) represents porous tantalum *in vivo* for 12 weeks with Van Gieson's stain. Dc: dense connective tissue; Lc: loose connective tissue. Big image was magnified 100 ×; small image was magnified 400×. (A color version of this figure is available in the online journal.)

equivalent to mature bone in the pore of tantalum rods was observed on defect sites (Figure 6(f)). In bone defect animals without treatment, massive fibrillar connective tissue was observed at 12 weeks (Figure 6(g)) while some new osteoblast was observed in the defect margins at 12 weeks post-BMSCs implantation (Figure 6(h)). Surgery process was shown in canine greater trochanter window with porous tantalum rod implantation (Figure 6(j)). Figure 6(k) shows the X-ray imaging of porous tantalum implanted into the cancellated bone tissue. Statistical results showed that at the same time point of postimplantation, porous tantalum rods associated with autologous BMSCs could accelerate the formation of new bone in the pores (Figure 7).

Discussion

The major finding of this work is two-folds: (1) Newly developed tantalum coating and its scaffold have good osteoconduction and can promote adhesion, aggregation, and proliferation of BMSCs *in vitro*. (2) Tantalum coating of RVC supplemented with autologous BMSCs successfully repaired bone defects in dogs and well integrated with the surrounding bone tissue in a more efficient way compared to using domestic porous tantalum implantation alone. It is notable that the regenerated trabecular post domestic porous tantalum plus autologous BMSCs implantation in dogs is equivalent to mature bone.

Previous studies show that porous tantalum also has sufficient mechanical strength, while its elastic modulus is lower than cortical bone and higher than cancellous bone.[34] These properties of porous tantalum make the post-implantation stress shelter negligible and are conducive to bone remodeling.[35] Furthermore, due to the flexibility and ductility of porous tantalum, porous tantalum will undergo just slight deformation but without fragmentation when contacting the hard cortical bone *in vivo*. Moreover, it is beneficial to postimplantation initial stability for the host bone because of its large friction coefficient. Zimmer has produced porous tantalum for the first time and achieved good effectiveness for treating bone defect clinically.[21] In the last few years, there have been some research on the combination of porous tantalum and other biological materials to repair the osteochondral or cartilage defect. For example, porous tantalum in combination with periosteal grafts can promote excellent bony incorporation of the scaffold into trabecular subchondral bone.[36] Tantalum scaffold with fibrin as cell carrier promotes chondrocyte proliferation and cartilaginous tissue formation.[37] In addition, porous tantalum begins to be applied as dental implants in animal experiments and in clinic.[38,39]

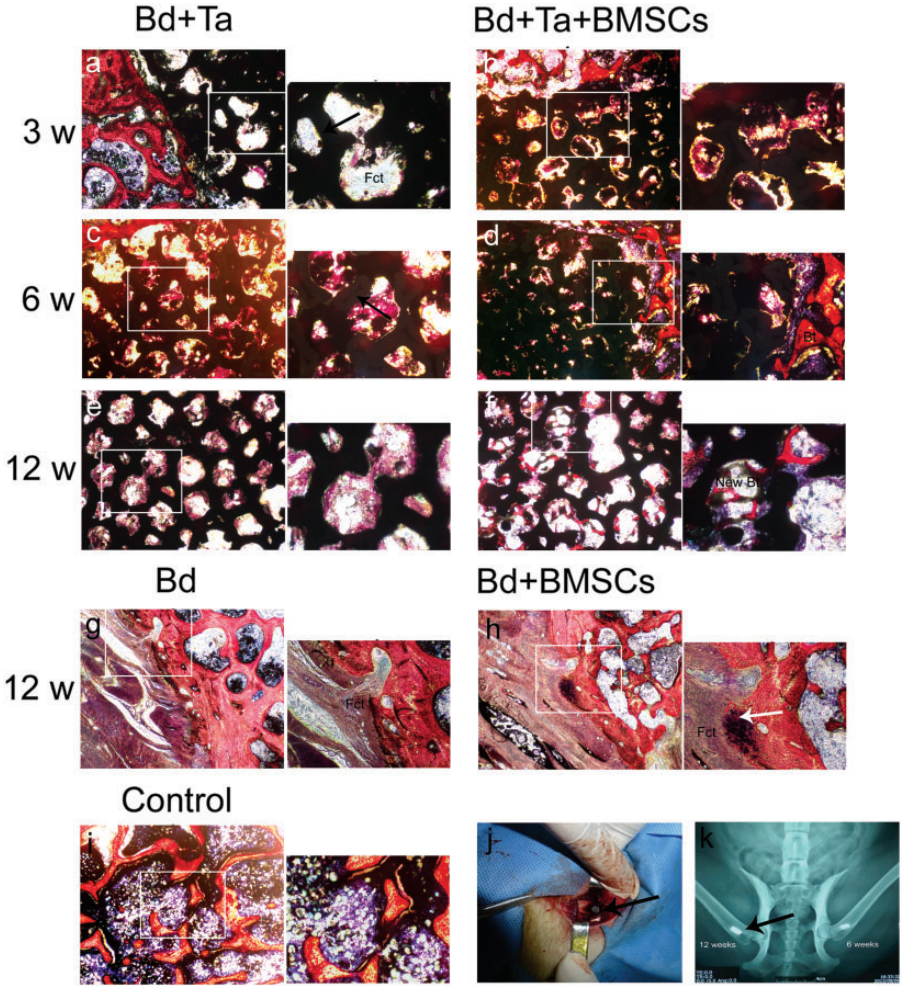

Figure 6 Osteogenesis of porous tantalum with or without BMSCs for bone defect in canine greater trochanter. Porous tantalums (black arrows) are associated with the voids left from the implant. Porous tantalum implanted dogs (a, c, e), porous tantalum with BMSCs implanted dogs (b, d, f), bone defect (g), bone defect with BMSCs (h), and representative microphotographs of canine greater trochanter from control (i) with Van Gieson's stain. Bt: bone trabecula; Fct: fibrillar connective tissue. Osteoblast (white arrows). Control: normal bone tissue. Surgery in canine greater trochanter with tantalum rod (arrows) for three, six, and 12 weeks (j). X-ray imageology showed that porous tantalum (arrows) implanted cancellated bone (k)

Nevertheless, melting point of tantalum is about 3000°C, so porous tantalum with highly interconnected pores and uniform honeycomb structure is very difficult to obtain through the traditional technology. The preparation of porous tantalum was always a problem in the past decades. Zimmer produces tantalum coating on thermosetting polymer foam precursor by chemical vapor deposition and becomes the only medical device company with porous tantalum in the world. However, the product is very expensive, and the widespread use of porous tantalum in China is limited. Wang *et al.* prepared porous tantalum by the powder metallurgy technique and implanted into the femoral condyle of rabbits.[40] But this method is difficult to get high open-cell porous metals. In recent years, with the rapid development of 3D printing technology, net-shape porous tantalum has been created with laser engineered net shaping technique and applied for bone defects in rat.[41] One question is that the spherical pure tantalum powder for 3D printing costs so much and very difficult to purchase. At present, the most effective method is to use chemical vapor deposition technique to prepare tantalum coating on three-dimensional scaffold, such as porous Ti6Al4V scaffold.[42] With a long-term period of research and development, we have successfully made out tantalum coating on the surface of domestic porous RVC scaffold using chemical vapor deposition technique in China for the first time.

It has been several decades that carbon is used in medicine field. RVC characterized by light weight and low density has highly interconnected pores and honeycomb structure. Wickham and Kent, respectively, reported favorable properties of RVC as a matrix for corneal endothelial cells or embryo fibroblast 3T6 cells growth.[43,44] Pec *et al.* found that their RVC bought from Oakland, United States was cytotoxic for rabbit MSCs but not for rabbit chondrocytes.[24] In this work, we confirmed that there was no cytotoxicity for domestic RVC co-cultured with canine BMSCs. Meanwhile, confocal laser microscope and dynamic observation with SEM both showed more and more adherent and fully spread BMSCs appearing on the surface of RVC and in the pore of RVC. All of these proved that our RVC biomaterial was much safer. However, RVC is very brittle and easy to crack because of its low mechanical strength. In

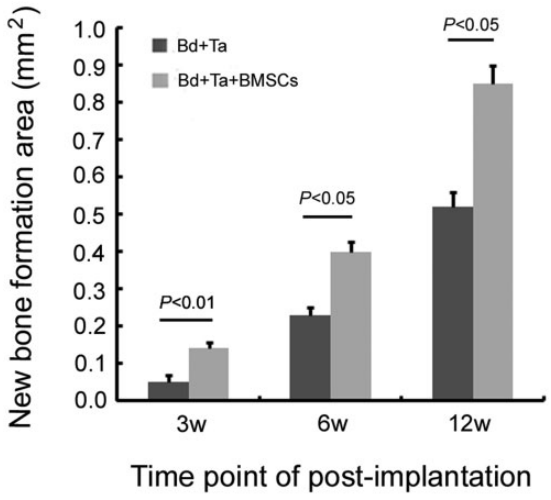

Figure 7 New bone formation area in the pores of porous tantalum. Five visual fields on each slice were selected randomly and taken pictures under 100× magnification optical microscope. New bone formation area in the pores of porous tantalum was measured by Image J software. Statistical results showed that at the same time point of postimplantation, porous tantalum rods associated with autologous BMSCs could accelerate the formation of new bone in the pores ($n = 3$)

the clinical practice, RVC is usually considered as a kind of scaffold in order to provide three-dimensional structure. So, there is no need to perform experiments demonstrating the potential effects of RVC implantation *in vivo*.

No matter *in vivo* or *in vitro*, cells and tissues will first contact with the surface of material. So it is very important for the cells to adhere the material surface as the first step. The different adhesion properties of different materials can largely affect cells proliferation and differentiation. Excellent proliferation, adhesion, and spread of BMSCs on this newly developed porous tantalum were assessed by MTT and SEM *in vitro*. Meanwhile, SEM results showed that the three-dimensional porous structure of the tantalum promoted secretion and infiltration of nutrients and metabolites. All of these demonstrate that domestic porous tantalum had excellent biocompatibility.

It is well known that massive fibrillar connective tissue will be generated around the defect sites for large-area bone defect. To observe the good biocompatibility of tantalum coating with loose connective tissue and dense connective tissue, porous tantalum was implanted into subcutaneous pocket under the canine groin. After 12 weeks, porous tantalum was surrounded by the connective tissue without local tumorigenesis and inflammatory reaction. Hacking *et al.* also found that porous tantalum of subcutaneous implants permitted rapid ingrowth of vascularized soft tissue and attained soft tissue attachment strengths greater than with porous beads.[45] This result was consistent with ours. Moreover, Ren *et al.* reported that porous tantalum cylinder was beneficial to the treatment of bone defects suffered from firearm injuries in rabbit.[46] In this work, the osteogenic potential of porous tantalum associated with autologous BMSCs was detected. We found that the efficacy of co-implantation with porous tantalum and autologous BMSCs was much better than porous tantalum implantation alone at comparable time point postimplantation. In proportion with implantation time (3w, 6w, 12w), more and more new bone tissue grew at the interface of the tantalum and the host bone, on the surface of the tantalum coating and in the pores. Three-dimensional structure and interconnected pores of sufficient size were beneficial for bone cell adhesion and migration and appropriate for osteogenesis. Interestingly, regenerated trabecular equivalent to mature bone in the pore of tantalum rods was evidenced at the implanted defect site after 12 weeks implantation of porous tantalum rods with autologous BMSCs. Taken together, abovementioned results suggest that the newly developed domestic porous tantalum with autologous BMSCs can be considered as an ideal bone trabecula substitution for clinical use. In large-area bone defect animals without treatment, massive fibrillar connective tissue was observed at 12 weeks, while some new osteoblast was observed in the defect margins at 12 weeks post-BMSCs implantation. We hypothesized that implanted BMSCs might differentiate into osteoblasts.

In summary, we found that newly developed domestic tantalum coating and its scaffold can promote adhesion, aggregation, and proliferation of BMSCs *in vitro*. *In vivo* studies demonstrate that implanted tantalum with a high porosity (70–85%) and host bone may produce a stable connection and integration. The osteogenic potential of domestic porous tantalum associated with autologous BMSCs is excellent and regenerated trabecular equivalent to mature bone in the pore of tantalum. Future clinical studies are warranted to verify the clinical efficacy of combined implantation of this domestic porous tantalum plus BMSCs implantation and compare their efficacy with conventional autologous bone grafting carrying blood vessel in patients needing bone repairing.

Authors' contributions: XW and DZ conceived and designed the experiments, XW, KK, and HX performed the experiments, BW and WW analyzed the data, JZ and ZY contributed materials/analysis tools, XW wrote the paper, BL and XZ revised the manuscript and interpreted the results.

ACKNOWLEDGEMENTS

We thank Dr Yuejian Liu for technical assistance. We thank Dr Kai Hu from Würzburg University for his help on the preparation of this manuscript. The project was supported by the National Natural Science Foundation of China (No. 81371942), National Science and Technology Support Program (2012BAI17B02), Dalian Science and Technology Bureau (No. 2013J21DW004) and Dalian University (No. 2015YBL003).

DECLARATION OF CONFLICTING INTERESTS

The author(s) declared no potential conflicts of interest with respect to the research, authorship, and/or publication of this article.

REFERENCES

1. DeCoster TA, Gehlert RJ, Mikola EA, Pirela-Cruz MA. Management of posttraumatic segmental bone defects. *J Am Acad Orthop Surg* 2004;**12**:28–38
2. Nishida J, Shimamura T. Methods of reconstruction for bone defect after tumor excision: a review of alternatives. *Med Sci Monit* 2008;**14**:RA107–13
3. Bosch C, Melsen B, Vargervik K. Importance of the critical-size bone defect in testing bone-regenerating materials. *J Craniofac Surg* 1998;**9**:310–6
4. Aurégan JC, Bégué T. Induced membrane for treatment of critical sized bone defect: a review of experimental and clinical experiences. *Int Orthop* 2014;**38**:1971–8
5. Kinaci A, Neuhaus V, Ring DC. Trends in bone graft use in the United States. *Orthopedics* 2014;**37**:e783–8
6. Carulli C, Innocenti M, Brandi ML. Bone vascularization in normal and disease conditions. *Front Endocrinol (Lausanne)* 2013;**4**:106
7. Jones JR, Lee PD, Hench LL. Hierarchical porous materials for tissue engineering. *Philos Trans A Math Phys Eng Sci* 2006;**364**:263–81
8. Jandali S, Diluna ML, Storm PB, Low DW. Use of the vascularized free fibula graft with an arteriovenous loop for fusion of cervical and thoracic spinal defects in previously irradiated pediatric patients. *Plast Reconstr Surg* 2011;**127**:1932–8
9. Wang B, Zhao D, Liu B, Wang W. Treatment of osteonecrosis of the femoral head by using the greater trochanteric bone flap with double vascular pedicles. *Microsurgery* 2013;**33**:593–9
10. Scott TG, Blackburn G, Ashley M, Bayer IS, Ghosh A, Biris AS. Advances in bionanomaterials for bone tissue engineering. *J Nanosci Nanotechnol* 2013;**13**:1–22
11. Li Z, Kawashita M. Current progress in inorganic artificial biomaterials. *J Artif Organs* 2011;**14**:163–70
12. Sehatzadeh S, Kaulback K, Levin L. Metal-on-metal hip resurfacing arthroplasty: an analysis of safety and revision rates. *Ont Health Technol Assess Ser* 2012;**12**:1–63
13. Findlay DM, Welldon K, Atkins GJ, Howie DW, Zannettino AC, Bobyn D. The proliferation and phenotypic expression of human osteoblasts on tantalum metal. *Biomaterials* 2004;**12**:2215–27
14. Sagomonyants KB, Hakim-Zargar M, Jhaveri A, Aronow MS, Gronowicz G. Porous tantalum stimulates the proliferation and osteogenesis of osteoblasts from elderly female patients. *J Orthop Res* 2011;**4**:609–16
15. Welldon KJ, Atkins GJ, Howie DW, Findlay DM. Primary human osteoblasts grow into porous tantalum and maintain an osteoblastic phenotype. *J Biomed Mater Res A* 2008;**3**:691–701
16. Nakashima Y, Mashima N, Imai H, Mitsugi N, Taki N, Mochida Y, Owan I, Arakaki K, Yamamoto T, Mawatari T, Motomura G, Ohishi M, Doi T, Kanazawa M, Iwamoto Y. Clinical and radiographic evaluation of total hip arthroplasties using porous tantalum modular acetabular components: 5-year follow-up of clinical trial. *Mod Rheumatol* 2013;**1**:112–8
17. Boureau F, Putman S, Arnould A, Dereudre G, Migaud H, Pasquier G. Tantalum cones and bone defects in revision total knee arthroplasty. *Orthop Traumatol Surg Res* 2015;**2**:251–5
18. Budge MD, Nolan EM, Heisey MH, Baker K, Wiater JM. Results of total shoulder arthroplasty with a monoblock porous tantalum glenoid component: a prospective minimum 2-year follow-up study. *J Shoulder Elbow Surg* 2013;**4**:535–41
19. Sagherian BH, Claridge RJ. Porous tantalum as a structural graft in foot and ankle surgery. *Foot Ankle Int* 2012;**3**:179–89
20. Hanc M, Fokter SK, Vogrin M, Molicnik A, Recnik G. Porous tantalum in spinal surgery: an overview. *Eur J Orthop Surg Traumatol* 2015;**26**:1–7
21. Levine BR, Sporer S, Poggie RA, Della Valle CJ, Jacobs JJ. Experimental and clinical performance of porous tantalum in orthopedic surgery. *Biomaterials* 2006;**27**:4671–81
22. Vardharajula S, Ali SZ, Tiwari PM, Eroğlu E, Vig K, Dennis VA. Functionalized carbon nanotubes: biomedical applications. *Int J Nanomedicine* 2012;**7**:5361–74
23. Qiu YS, Shahgaldi BF, Revell WJ, Heatley FW. Evaluation of Gateshead carbon fibre rod as an implant material for repair of osteochondral defects: a morphological and mechanical study in the rabbit knee. *Biomaterials* 2002;**23**:3943–55
24. Pec MK, Reyes R, Sánchez E, Carballar D, Delgado A, Santamaría J. Reticulated vitreous carbon: a useful material for cell adhesion and tissue invasion. *Eur Cell Mater* 2010;**20**:282–94
25. Aoki K, Usui Y, Narita N, Ogiwara N, Iashigaki N, Nakamura K. A thin carbon-fiber web as a scaffold for bone-tissue regeneration. *Small* 2009;**5**:1540–6
26. Cortes Y, Ojeda M, Araya D, Dueñas F, Fernández MS, Peralta OA. Isolation and multilineage differentiation of bone marrow mesenchymal stem cells from abattoir-derived bovine fetuses. *BMC Vet Res* 2013;**9**:133
27. Zhao D, Cui D, Wang B, Tian F, Guo L, Yang L, Liu B, Yu X. Treatment of early stage osteonecrosis of the femoral head with autologous implantation of bone marrow-derived and cultured mesenchymal stem cells. *Bone* 2012;**50**:325–30
28. Stiehler M, Lind M, Mygind T, Baatrup A, Dolatshahi-Pirouz A, Li H, Foss M, Besenbacher F, Kassem M, Bünger C. Morphology, proliferation, and osteogenic differentiation of mesenchymal stem cells cultured on titanium, tantalum, and chromium surfaces. *J Biomed Mater Res A* 2008;**2**:448–58
29. Grayson WL, Bunnell BA, Martin E, Frazier T, Hung BP, Gimble JM. Stromal cells and stem cells in clinical bone regeneration. *Nat Rev Endocrinol* 2015;**11**:140–50
30. Goessler UR, Riedel K, Hormann K, Riedel F. Perspectives of gene therapy in stem cell tissue engineering. *Cells Tissues Organs* 2006;**183**:169–79
31. Gao C, Harvey EJ, Chua M, Chen BP, Jiang F, Liu Y. MSC-seeded dense collagen scaffolds with a bolus dose of VEGF promote healing of large bone defects. *Eur Cell Mater* 2013;**26**:195–207
32. Behnia H, Khojasteh A, Kiani MT, Khoshzaban A, Mashhadi Abbas F, Bashtar M, Dashti SG. Bone regeneration with a combination of nanocrystalline hydroxyapatite silica gel, platelet-rich growth factor, and mesenchymal stem cells: a histologic study in rabbit calvaria. *Oral Surg Oral Med Oral Pathol Oral Radiol* 2013;**115**:e7–15
33. Lee RH, Kim B, Choi I, Kim H, Choi HS, Suh K, Bae YC, Jung JS. Characterization and expression analysis of mesenchymal stem cells from human bone marrow and adipose tissue. *Cell Physiol Biochem* 2004;**14**:311–24
34. Stiehler M, Lind M, Mygind T, Baatrup A, Dolatshahi-Pirouz A, Li H, Foss M, Besenbacher F, Kassem M, Bünger C. Morphology, proliferation, and osteogenic differentiation of mesenchymal stem cells cultured on titanium, tantalum, and chromium surfaces. *J Biomed Mater Res A* 2008;**86**:448–58
35. Tang Z, Xie Y, Yang F, Huang Y, Wang C, Dai K. Porous tantalum coatings prepared by vacuum plasma spraying enhance BMSCs osteogenic differentiation and bone regeneration in vitro and in vivo. *PLoS One* 2013;**8**:e66263
36. Mrosek EH, Schagemann JC, Chung HW, Fitzsimmons JS, Yaszemski MJ, Mardones RM, O'Driscoll SW, Reinholz GG. Porous tantalum and poly-epsilon-Caprolactone biocomposites for osteochondral defect repair: preliminary studies in rabbits. *J Orthop Res* 2010;**2**:141–8
37. Jamil K, Chua KH, Joudi S, Ng SL, Yahaya NH. Development of a cartilage composite utilizing porous tantalum, fibrin, and rabbit chondrocytes for treatment of cartilage defect. *J Orthop Surg Res* 2015;**10**:27
38. Liu Y, Bao C, Wismeijer D, Wu G. The physicochemical/biological properties of porous tantalum and the potential surface modification techniques to improve its clinical application in dental implantology. *Mater Sci Eng C Mater Biol Appl* 2015;**49**:323–9
39. Lee JW, Wen HB, Battula S, Akella R, Collins M, Romanos GE. Outcome after placement of tantalum porous engineered dental implants in fresh extraction sockets: a canine study. *Int J Oral Maxillofac Implants* 2015;**1**:134–42
40. Wang Q, Zhang H, Li Q, Ye L, Gan H, Liu Y, Wang H, Wang Z. Biocompatibility and osteogenic properties of porous tantalum. *Exp Ther Med* 2015;**3**:780–6

41. Wauthle R, van der Stok J, Amin Yavari S, Van Humbeeck J, Kruth JP, Zadpoor AA, Weinans H, Mulier M, Schrooten J. Additively manufactured porous tantalum implants. *Acta Biomater* 2015;**14**:217–25
42. Li X, Wang L, Yu X, Feng Y, Wang C, Yang K, Su D. Tantalum coating on porous Ti6Al4V scaffold using chemical vapor deposition and preliminary biological evaluation. *Mater Sci Eng C Mater Biol Appl* 2013;**5**:2987–94
43. Wickham MG, Cleveland PH, Binder PS, Akers PH. Growth of cultured corneal endothelial cells onto a vitreous carbon matrix. *Ophthalmic Res* 1983;**15**:116–20
44. Kent BL, Mutharasan R. Cultivation of animal cells in a reticulated vitreous carbon foam. *J Biotechnol* 1992;**22**:311–27
45. Hacking SA, Bobyn JD, Toh K, Tanzer M, Krygier JJ. Fibrous tissue ingrowth and attachment to porous tantalum. *J Biomed Mater Res* 2000;**4**:631–8
46. Ren B, Zhai Z, Guo K, Liu Y, Hou W, Zhu Q, Zhu J. The application of porous tantalum cylinder to the repair of comminuted bone defects: a study of rabbit firearm injuries. *Int J Clin Exp Med* 2015;**8**:5055–64

(Received September 16, 2015, Accepted January 4, 2016)